

Thermal Diffuse Scattering within a Bragg Peak*

BY HELLMUT J. JURETSCHKE

Polytechnic Institute of New York, 333 Jay Street, Brooklyn, New York 11201, USA

(Received 31 August 1984; accepted 10 July 1985)

Abstract

The dynamical theory of X-ray-phonon interactions for one-phonon processes is applied to find the thermal diffuse scattering for incident radiation within the angular region of a Bragg peak. In this region contributions must be included from phonons that do not obey the traditional selection rule of connecting points on the two-beam dispersion surface. The general result is evaluated explicitly for the Ge 220 symmetric reflection. The thermal diffuse scattering distribution in output angle is strongly suppressed in the central region, and shows peaks close to the edges of this region as well as at the direction of specular reflection. The suppression of the interaction, and the appearance of the pseudospecular peak, can be traced to the large primary extinction for both the incident and outgoing beams in this region, in addition to the boundary condition that the phonon-excited signal be entirely internally generated. Both effects also combine to eliminate the traditionally expected divergence of thermal diffuse scattering at the Bragg peak.

1. Introduction

The interaction of X-rays with thermal phonons (TDS) in the angular region of nearly total reflection of a Bragg peak is of both practical and theoretical interest. It is needed for an accurate determination of structure factors, as a correction to the experimentally measured intensities that cannot differentiate between elastic and inelastic scattering in this region (Cochran, 1969). Furthermore, simple scattering theory predicts that the cross section for this interaction diverges as the scattering vector \mathbf{Q} , defined by

$$\mathbf{Q} = \mathbf{K}_f - \mathbf{K}_0 = \mathbf{H} + \mathbf{q}, \quad (1)$$

approaches a reciprocal-lattice vector \mathbf{H} when the phonon wave vector \mathbf{q} goes to zero (Willis & Pryor, 1975). While integrable, this divergence enhances the contribution of very-long-wavelength phonons ($\lambda = 2\pi/q$) beyond their actual population density, and deserves, for this and for more formal reasons, more detailed scrutiny.

* Supported in part by the Joint Services Electronics Program Contract No. F49620-82-C-0084.

In contrast to X-rays, the diffraction of γ -rays using Mössbauer techniques allows an energy discrimination sufficient to separate elastic scattering and inelastic TDS in the region of the Bragg peak. It has been shown (O'Connor & Butt, 1963) that instead of diverging, or reaching a plateau, TDS actually shows a dip in the central portion of this region. The dip is replaced by a shallow maximum as the crystal quality in the surface region deteriorates. Both of these features are consistent with these authors' explanation that the strong primary extinction of perfect crystals in the Bragg region limits the depth of the interaction of X-rays with phonons severely enough to overcome any divergent trends. More recently, similar results have been obtained using X-rays (Kashiwase, Kainuma & Minoura, 1982). A defect line normal to the plane of incidence was found in the TDS. This line persisted even as the incident direction traversed the Bragg angle, and was attributed to Bragg scattering of phonons. The same phenomenon has now received a more detailed geometrical explanation in terms of the similar behavior of Kikuchi lines in electron diffraction (Wilkins, Chadderton, & Smith, 1983).

Without categorizing these effects in detail, we have been using a dynamical theory of X-ray phonon interaction in perfect crystals (Wasserstein-Robbins & Juretschke, 1985) to show that such defect lines should indeed exist, and that they have two major causes. Firstly, primary extinction plays exactly the role of limiting the depth of interaction suggested by O'Connor & Butt (1963). Secondly, there is the boundary condition requiring that the emerging phonon-excited signal is entirely generated within the crystal. This becomes important in specifying the Bragg-diffracted fields when the phonon-excited X-ray modes are composed of two coherent fields of comparable magnitude, as is the case within and in the immediate vicinity of the region of total reflection. While our companion paper (Wasserstein-Robbins & Juretschke, 1985), hereafter designated WJ, presents a general formulation of TDS for all one-phonon transitions, the results explicitly discussed there have been limited to the situations where the angle of incidence θ_{in} relative to the Bragg angle θ_B is large compared to the angular width of total reflection, *i.e.* $|\theta_{in}| \gg |TF_H|$. The present paper extends the explicit

results to cover all values of θ_{in} , and in particular those lying within the region of total reflection. Earlier treatments of this problem by O'Connor (1967) and Afanas'ev, Kagan & Chukovskii (1968) have developed the general approach also used here, but, as pointed out in WJ, did not include a sufficiently complete handling of the boundary condition to permit quantitative exploration of this central region.

The dynamical theory of WJ treats X-ray phonon scattering by using as a starting point the dynamical solutions of X-ray modes in perfect crystals (e.g. Batterman & Cole, 1964). Phonons, with lifetimes long compared to the passage of X-ray photons through the crystal, essentially impose a spatial modulation on all structure factors, which set up new normal modes of X-ray propagation within the crystal (e.g. Köhler, Möhling & Peibst, 1970). In the approximation limited to single-phonon processes, N phonons will set up a system of $2N+1$ modes, with each mode containing $2(2N+1)$ coherent fields (O'Connor, 1967; Afanas'ev *et al.*, 1968; Köhler, Möhling & Peibst, 1974; Wasserstein-Robbins, 1982). In consonance with the general spirit of dynamical theory (Ewald, 1916), TDS is then obtained by determining the excitation of phonon-coupled modes in addition to the central elastic, *i.e.* phonon-free, mode that results when a single external field is incident on the crystal. As already mentioned, this excitation is partly controlled by the condition that the net incident fields for all but the central field direction must vanish. A particular example using this approach, for $N=1$, and leading to a six-beam problem, has been examined (Juretschke & Wasserstein-Robbins, 1982) for phonons traveling parallel to the surface. It has an exact analytic solution for arbitrarily large phonon intensities (within the one-phonon process approximation) that can serve as a yardstick for examining the limits of approximate solutions.

For thermal phonons, where phonon intensities, proportional to $k_B T$, are weak, a solution restricted to the first power in $k_B T$ provides the most important contribution to TDS, and can be obtained by a perturbation expansion. Within this approximation, the TDS following from the general theory of WJ shows several specific features characteristic of the dynamical treatment: (a) For given angles θ_{in} of the incident field and θ_{out} of the inelastically reflected field the relevant phonon wave vector \mathbf{q}_0 is that connecting the two tiepoints on the *dynamical* two-beam dispersion surface (real part) that correspond to θ_{in} and θ_{out} . Therefore, wherever the dynamical and kinematical dispersion surfaces differ, such as in the region of strong reflection, the dynamically and kinematically expected phonons in TDS can differ in both magnitude and direction. (b) The overall TDS intensity is inversely proportional to the average absorption coefficient, *i.e.* it depends on the depth of penetration controlling the effective volume of X-ray phonon

interaction. (c) Wherever absorption differs from its average, at θ_{in} or θ_{out} , the relative coupling strength f varies accordingly. For example, if we fix θ_{in} as outside the reflecting region and let θ_{out} increase from negative to positive values through this region, f first increases as the crystal becomes anomalously transparent, and then drops sharply as the primary extinction becomes large. This drop in f largely accounts for the defect lines discussed earlier. Similarly, the asymptotic value of f as θ_{out} goes far away from zero is determined by the absorption at θ_{in} .

Strictly speaking, these features, based on the physically plausible separation into a relevant q_0 and an effective coupling strength f , describe TDS only when θ_{in} is outside the region of total reflection. As shown in WJ, in that case the sum over all phonons contributing to TDS for given θ_{in} and θ_{out} is dominated by the q_0 described under (a) above, and thus leads formally to the commonly accepted selection rule for momentum conservation in X-ray phonon interaction. Actually, when condition (1) is applied to the proper dispersion surface of $2N+1$ sheets needed to describe N phonons, other q 's also contribute to TDS. Only when θ_{in} is outside the Bragg-peak region is this contribution weighted by a Lorentzian sharply peaked at the conventional q_0 . On the other hand, when θ_{in} and θ_{out} are small this Lorentzian becomes broad and the contribution from the other q 's must be evaluated more carefully. This aspect of the problem was not taken up in WJ.

The generalized phonon contribution to TDS, and its consequences, are addressed below. § 2 presents a formal solution to the problem. § 3 applies the theory to the 220 reflection in Ge, and § 4 discusses some implications of these results for the general problem of X-rays interacting with long-wavelength phonons in diffracting regions.

2. Theory

The basic theoretical formulation of TDS, developed and discussed in WJ, will not be repeated here, but will be referred to extensively. To facilitate these references, equations from that paper will be cited with a prefaced WJ, *e.g.* (WJ-5). The formulation uses a formalism of dynamical theory adapted from that of Batterman & Cole (1964).

Our starting point is equation (WJ-20). As pointed out in WJ in connection with that equation, a fixed set (θ_{in} , θ_{out}) completely determines all the variables ξ that establish the tiepoints on all sheets of the dispersion surface of the participating modes. Hence, when summing (WJ-20) over all participating phonons, the only variable is the component q_z of all the phonon wave vectors having a common value of q_z . This variable, or its equivalent Δ_0 related to q_z through (WJ-13), appears explicitly in the denominator of (WJ-20), and also implicitly in the

factor $|F_{jH}F_{j\bar{H}}|$. By inserting in this factor the expression appropriate to thermal phonons, along the lines of WJ, we can write the generalization of f/q_0 as an average:

$$\begin{aligned} \langle f/q_0 \rangle = & \delta'' \{ [\xi'_{0H}(0) - \xi'_{j0}(j)]^2 \\ & + [\xi''_{0H}(0) - \xi''_{j0}(j)]^2 \} / |\xi_{0H}(0)|^2 \\ & \times \pi^{-1} \int_{-\infty}^{\infty} [q(\Delta_0, \Delta_H)]^{-1} \{ [\Delta_0 - \xi'_{jH}(j)] \\ & + \xi'_{00}(0) \}^2 + [\xi''_{00}(0) - \xi''_{jH}(j)]^2 \}^{-1} d\Delta_0. \quad (2) \end{aligned}$$

Here $\delta'' = k\Gamma F_0''$ measures the average absorption, and the ξ 's designate the tiepoints on the dispersion surface for θ_{in} and θ_{out} (see WJ). As expected, when the real part of $\xi_{00}(0) - \xi_{jH}(j)$ is much larger than the imaginary part, the second factor in the integral is a sharply peaked Lorentzian that can be replaced by a delta function. Under that condition, (2) reduces to f/q_0 of WJ. More generally, the integral expression in (2) has to be evaluated exactly, including the variation of the first factor.

For an arbitrary phonon in the plane of incidence, $q(\Delta_0, \Delta_H)$ is a function of the two independent variables Δ_0 and Δ_H , defined in (WJ-13) and corresponding to q_x and q_z :

$$q^2 = (\sin^2 2\theta_B)^{-1} \{ \Delta_0^2 + \Delta_H^2 - 2\Delta_0\Delta_H \cos 2\theta_B \}. \quad (3)$$

But if the variable q is to connect a fixed θ_{in} to the common θ_{out} , Δ_H is related to Δ_0 by the condition

$$\Delta_H = [\xi'_{j0}(j) - \xi'_{0H}(0)] + [\xi'_{jH}(j) - \xi'_{00}(0) - \Delta_0] \quad (4)$$

so that $q(\Delta_0, \Delta_H)$ in (2) is a function of Δ_0 only.

With the new variable

$$x = [\xi'_{jH}(j) - \xi'_{00}(0) - \Delta_0]$$

and the new constants

$$A = |\xi''_{00}(0) - \xi''_{jH}(j)|$$

$$C = \frac{1}{2} \{ \xi'_{j0}(j) + \xi'_{jH}(j) - [\xi'_{00}(0) + \xi'_{0H}(0)] \} \tan \theta_B$$

$$D = \frac{1}{2} \{ \xi'_{jH}(j) - \xi'_{j0}(j) - [\xi'_{00}(0) - \xi'_{0H}(0)] \}$$

the second factor of (2) can be rewritten as

$$(\sin \theta_B / \pi) \int_{-\infty}^{\infty} [(x - D)^2 + C^2]^{-1/2} (x^2 + A^2)^{-1} dx. \quad (5)$$

A convenient form for expressing this integral, which takes into account that different relative values of A , C and D lead to different formulations in terms of real functions, is given by

$$\begin{aligned} & (\sin \theta_B / \pi) (2/A) \operatorname{Im} \{ [(D - iA) \cosh z]^{-1} \\ & \times \{ \tanh^{-1} [(1 + \sinh z) / \cosh z] \\ & + \tanh^{-1} [(1 - \sinh z) / \cosh z] \} \}, \quad (6) \end{aligned}$$

where $\sinh z = C/(D - iA)$.

Of course, in evaluating (6) the proper relative phase angles of the multivalued function \tanh^{-1} of

complex argument must be observed. For example, in the asymptotic region $|A/D| \ll 1$, the imaginary parts of the arguments of the two \tanh^{-1} approach zero, but are of opposite sign. Hence the sum of the two \tanh^{-1} approaches $\pi/2$. Since in that same limit $D \cosh z$ approaches $(C^2 + D^2)^{1/2}$, and since this expression is also equal to $q_0 \sin \theta_B$, (6) becomes $1/(Aq_0)$. Then (2) is identical with the value f/q_0 of WJ, where, because θ_{in} is restricted to be large, we are always in this asymptotic limit. More generally, the same limit holds for arbitrary θ_{in} as long as $|\theta_{out}| \gg |\theta_{in}|$. If we now let θ_{out} vary and approach θ_{in} , the phase angles deriving from the imaginary parts of the \tanh^{-1} change continuously, except at $\theta_{in} = \theta_{out}$, where the constant C changes sign, and the two \tanh^{-1} interchange in value. This interchange introduces a qualitatively new feature in the behavior of (6) near $\theta_{in} = \theta_{out}$, not present in the asymptotic form used in WJ, which will be demonstrated and discussed below.

3. Results

Some of the contents of (6) will be explored by evaluating it explicitly for the symmetric 220 reflection of Ge, under Cu $K\alpha$ radiation. This allows continuity and direct comparison with the results shown in WJ, where the asymptotic form of (6), f/q_0 , was given for the same reflection at $\theta_{in} = \pm 70^\circ$.

For reference, and in order to put our results in perspective, we show in Fig. 1, for the Ge 220 reflection, the real part of the dispersion surface in $k_x - k_z$ space, and also the imaginary part of k_z , $|\mathcal{K}_z|$, that measures the primary extinction. The lower part of Fig. 1 includes the elastically reflected relative

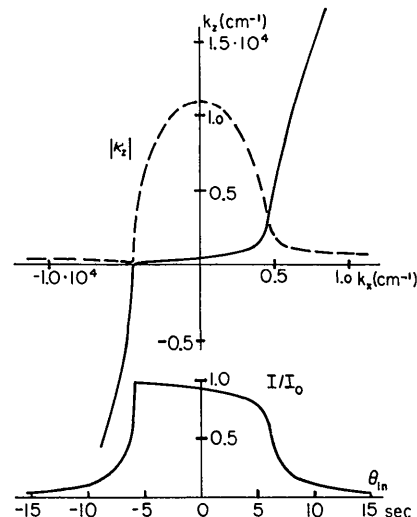


Fig. 1. General characteristics of the Ge 220 reflection (Cu $K\alpha$). Solid curve: real part of the normal branch of the dispersion surface (σ polarization). Dashed curve: imaginary part of k_z , $|\mathcal{K}_z|$. Insert below: relative elastically reflected intensity vs θ . The θ scale matches the k_x scale above it.

intensity I/I_0 , as a function of $\theta_{in}(=\theta_{out})$, with the θ scale corresponding to the k_x scale of the dispersion curves. $|\mathcal{K}_z|$ exhibits the typical maximum in the region of nearly total reflection, and the minimum just below $\theta = -6''$ where anomalous transmission occurs. The real part of the dispersion curve shows a strong deviation from the kinematic straight line through the origin at the angle $\cos^{-1}(22.65^\circ)$. All the values of ξ'_0 and ξ'_H entering into (6) are derived from this curve by

$$\begin{aligned}\xi'_0 &= -k_x \cos \theta_B + k_z \sin \theta_B, \\ \xi'_H &= -k_x \cos \theta_B - k_z \sin \theta_B\end{aligned}$$

and the imaginary parts by

$$\begin{aligned}\xi''_0 &= \mathcal{K}_z \sin \theta_B + \frac{1}{2}k\Gamma F''_0, \\ \xi''_H &= -\mathcal{K}_z \sin \theta_B + \frac{1}{2}k\Gamma F''_0.\end{aligned}$$

Fig. 2 shows the value of $\langle f/q_0 \rangle$ derived from (6) for $\theta_{in} = 10''$, which is still outside the main angular region of reflection of Fig. 1. The dashed curve in this figure is the result predicted for f/q_0 according to (WJ-23) and (WJ-25). Obviously, this asymptotic formula is still very good. Compared to Fig. 5 of WJ for $\theta_{in} = 70''$, the maximum amplitude is about seven times larger, in agreement with a reduction of θ_{in} by the same factor, and therefore reflecting the typical $1/q_0$ dependence. In both the asymptotic curve and the exact result the maximum near $\theta_{out} = \theta_{in}$, pronounced in Fig. 5 of WJ, is now reduced relative to that near $\theta_{out} = -\theta_{in}$. In addition, there is a new feature near $\theta_{out} = 10'' (= \theta_{in})$, in terms of a new peak superimposed on the smooth f/q_0 curve. This peak, in fact, shows a weak divergence, at the exact angle of specular reflection, which is probably largely due to the use of first-order solutions based on the unperturbed dispersion surface, in WJ and in this paper. But apart from this spurious divergence at exactly

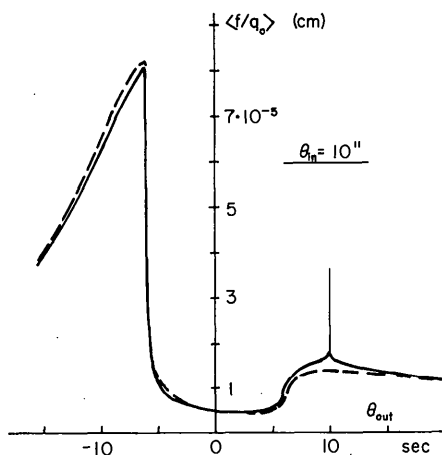


Fig. 2. Comparison of f/q_0 of WJ (dashed curve) and $\langle f/q_0 \rangle$ of (6) vs θ_{out} , for $\theta_{in} = 10''$, for the reflection of Fig. 1. $\langle f/q_0 \rangle$ exhibits a new peak around $\theta_{out} = \theta_{in}$.

$\theta_{out} = \theta_{in}$, the new peak persists at neighboring values of θ_{out} where this solution is good. Such a peak around the elastic scattering output angle has already been found in an exact solution of another configuration of X-ray phonon interactions (Juretschke & Wasserstein-Robbins, 1982), although it has never yet been identified experimentally. It is a direct consequence of the boundary condition imposed on the net field of all phonon excited modes. The deep minimum in the region $|\theta_{out}| < 6''$ in Fig. 2 is the dynamical suppression of the phonon interaction because of primary extinction, in both f/q_0 and $\langle f/q_0 \rangle$.

Fig. 3 extends the results for $\langle f/q_0 \rangle$ to the edge of the region of total reflection, with $\theta_{in} = \pm 7''$. The behavior already described for Fig. 2 persists, with the new peaks around $\theta_{out} = \theta_{in}$ gaining in prominence. The combination of this peak and the minimum in primary extinction near $\theta_{out} = -7''$ gives the interaction at negative incident angles increased weight. The maxima of $\langle f/q_0 \rangle$ are still increasing, but, except in the region of the new peak, $\langle f/q_0 \rangle$ lies between 10 and 40% below f/q_0 (not shown), mostly so in the region of total reflection.

Fig. 4 carries the results fully into this region. At $\theta_{in} = \pm 5''$, the central minimum, now higher than in Fig. 3, is surrounded by peaks of similar heights remaining at the edges of the reflecting region. For $\theta_{in} = 0''$ the central minimum is replaced by the new pseudoelastic peak, but shoulders of the other two peaks persist at the same edge locations of θ_{out} as for $\theta_{in} = \pm 5''$. In the central region the magnitude of $\langle f/q_0 \rangle$ for $\theta_{in} = 0''$ is down by a factor of about five from the asymptotic expectation f/q_0 , indicating that in this region the proper evaluation of (6) is essential for predicting the correct TDS.

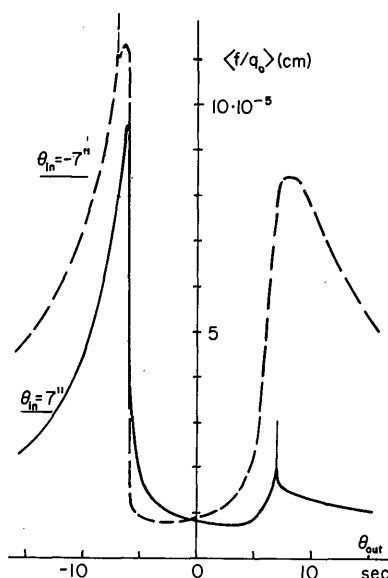


Fig. 3. $\langle f/q_0 \rangle$ vs θ_{out} for $\theta_{in} = \pm 7''$, just outside the main reflecting region of Fig. 1.

Most of these features are a quantitative confirmation of the behavior anticipated by O'Connor (1967), although not fully contained in his formulation. Of course, higher-order effects due to thermal distortion of the dispersion surfaces have not been included here.

4. Discussion

In order to compare these theoretical results with any specific experiment, such as that of O'Connor & Butt (1963), we would have to convolute the incident beam width with a series of functions of the form shown in Figs. 2 to 4. However, even without this, we can draw several conclusions about TDS in the Bragg region, valid for arbitrary incident beam profiles.

First of all, TDS is strongly suppressed in the angular region of total reflection, regardless of θ_{in} . Hence, wherever elastic and inelastic scattering can be separated, we expect a defect line normal to the plane of incidence, and centered around $\theta_{out}=0''$. This is in full accord with the observations of O'Connor & Butt (1963) and Kashiwase, Kainuma & Minoura (1982). We must assume, of course, that in these experiments the crystals were perfect enough so that dynamical processes operate fully. On the other hand, any gross divergence of the incident beam would at most produce a superposition of the effects discussed here, and those taken up in WJ, without obscuring the defect line. In any case, our results indicate that, in high-resolution experiments on perfect crystals, the TDS contribution to the Bragg intensity is considerably more complex than usually assumed.

The physical reasons for the suppression of TDS have already been explained, in terms of a combina-

tion of a number of effects. When both θ_{in} and θ_{out} are in the Bragg region, these can no longer be separated. However, an interesting new conceptual insight emerges from the evaluation of (2) given in §3: Whenever $\langle f/q_0 \rangle$ differs from f/q_0 , it is not sufficient to use the traditional selection rule that the \mathbf{q} of the relevant phonon producing coupling must connect two tiepoints on the two-beam dispersion surface. Tiepoints involving the same θ_{in} and θ_{out} , but off this dispersion surface, are also active, and their \mathbf{q} 's contribute to the total TDS. In particular, they also produce the pseudospecular peak that gives the TDS a nearly symmetric appearance at small input angles, such as in Fig. 4. The formal reason for this breakdown of the traditional selection rule, already discussed in WJ, is that actually a $2N+1$ sheeted dispersion surface is needed to describe the totality of single-phonon processes.

Secondly, the results of Figs. 2 to 4 show that the traditionally expected divergence of TDS, associated with the $1/q_0$ dependence of this interaction, does not occur in a fully dynamical theory. Judging from these figures, the $1/q_0$ dependence holds only as long as both θ_{in} and θ_{out} lie outside the edges of the region of total reflection, here given by $\pm 6''$, as indicated in Fig. 1. Inside this region, primary extinction and the other effects take over. Of course, because of the dispersion surfaces' deviation from straight lines in this region, as seen in Fig. 1, q_0 cannot vanish at $\theta=0''$, but rather does so at the crossover of the dispersion curve and the k_x axis, here occurring at θ close to $-5.72''$. At exactly that angle, the smallest classical phonon connects $\theta_{out}=\theta_{in}$ with a propagation vector $q_0=0.635\text{ cm}^{-1}$ (or $\lambda\sim 10\text{ cm}$), so that $1/q_0\approx 1.6\text{ cm}$. Yet $\langle f/q_0 \rangle$, as calculated from (6), is only 0.4 pm , in agreement with the general magnitudes shown in Figs. 3 and 4 for nearby angles. Hence here dynamical effects suppress the X-ray-phonon interaction by a factor larger than 10^4 . It is also important to note that at this same angle the asymptotic estimate of WJ, using the classical selection rule for q_0 , gives $f/q_0=0.73\text{ mm}$, still more than a factor of 1000 larger than the full dynamical result. The origin of this large difference is that the very broad Lorentzian of (5) in this region gives an integral essentially proportional to $1/A^2$, or an interaction inversely proportional to the square of the absorption coefficient in the central region. [In quoting the value for $\langle f/q_0 \rangle$ above, we have eliminated the spurious weak divergence at $\theta_{out}=\theta_{in}$, occurring for all θ_{in} , which, as already discussed above, is most probably associated with the perturbation approximation underlying the starting expression (2). Since this divergence is extremely narrow, it does not appreciably distort the values of $\langle f/q_0 \rangle$ small fractions of a second of arc away.] Obviously, at values of q_0 as small as the one considered above, other effects such as sample size or low-frequency environmental noise

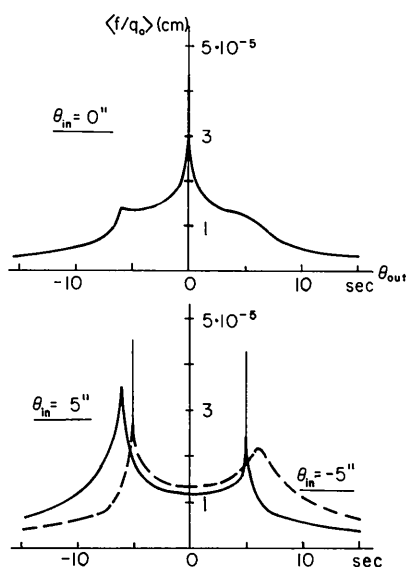


Fig. 4. $\langle f/q_0 \rangle$ vs θ_{out} for $\theta_{in} = \pm 5''$ and $\theta_{in} = 0''$, on the same scale as Figs. 2 and 3.

will severely distort the ideal interaction considered here. Such a suppression of the TDS divergence was not obtained by Afanas'ev *et al.* (1968), based on a somewhat different formulation that still led to a $\log(q)$ dependence. The differences in formulation have already been discussed in WJ.

Finally, dynamical modifications of the kind discussed here should also manifest themselves in the interaction of X-rays with other types of waves. Apart from any specific details of the interaction, the expression replacing $\langle f/q_0 \rangle$ will have to take into account that the density of states of these waves may differ from the $1/q$ dependence for thermal phonons underlying the form of (6).

References

- AFANAS'EV, A. M., KAGAN, Y. & CHUKOVSKII, F. N. (1968). *Phys. Status Solidi*, **28**, 287-294.
- BATTERMAN, B. W. & COLE, H. (1964). *Rev. Mod. Phys.* **36**, 681-717.
- COCHRAN, W. (1969). *Acta Cryst.* **A25**, 95-101.
- EWALD, P. P. (1916). *Ann. Phys. (Leipzig)*, **49**, 1-38.
- JURETSCHKE, H. J. & WASSERSTEIN-ROBBINS, F. (1982). *Phys. Rev. B*, **26**, 4262-4268.
- KASHIWASE, Y., KAINUMA, Y. & MINOURA, M. (1982). *Acta Cryst.* **A38**, 390-391.
- KÖHLER, R., MÖHLING, W. & PEIBST, H. (1970). *Phys. Status Solidi*, **41**, 75-80.
- KÖHLER, R., MÖHLING, W. & PEIBST, H. (1974). *Phys. Status Solidi B*, **61**, 173-180.
- O'CONNOR, D. A. (1967). *Proc. Phys. Soc.* **91**, 917-927.
- O'CONNOR, D. A. & BUTT, N. M. (1963). *Phys. Lett.* **7**, 233-235.
- WASSERSTEIN-ROBBINS, F. (1982). PhD Thesis, Polytechnic Institute of New York.
- WASSERSTEIN-ROBBINS, F. & JURETSCHKE, H. J. (1985). *Acta Cryst.* **A41**, 591-597.
- WILKINS, S. W., CHADDERTON, L. T. & SMITH, T. F. (1983). *Acta Cryst.* **A39**, 797-800.
- WILLIS, B. T. M. & PRYOR, A. W. (1975). *Thermal Vibrations in Crystallography*, ch. 7. Cambridge Univ. Press.

Acta Cryst. (1985). **A41**, 603-605

Reciprocal-Lattice Interpretation of the Interaction of Crystal-Monochromated X-radiation with a Small Single Crystal

BY A. McL. MATHIESON

Division of Chemical Physics, CSIRO, PO Box 160, Clayton, Victoria, Australia 3168

(Received 14 March 1985; accepted 15 July 1985)

Abstract

When dealing with X-radiation of two near wavelengths, λ_1 and λ_2 , from a crystal monochromator, M , incident on a small single crystal, c , interpretation of the interaction between the radiation and the specimen crystal is usually based on a single reciprocal lattice and two reflecting circles (spheres) of radii $1/\lambda_1$ and $1/\lambda_2$ whose centres do not coincide. If one uses the alternative Ewald construction of a single reflecting circle (sphere) of unit radius (which uniquely defines the specimen crystal location) and two reciprocal lattices mutually parallel but dimensionally scaled as $\lambda_1:\lambda_2$ and with displaced origins, then this allows a more ready appreciation of the special relationships between the dispersion of the specimen crystal and that of the monochromator as θ_c changes, in particular, when θ_c equals $\arctan(0.5 \tan \theta_M)$, $\arctan(0.6 \tan \theta_M)$ or θ_M .

To illustrate the interaction of a small single crystal with monochromated radiation corresponding to a wavelength band $\Delta\lambda = \lambda_2 - \lambda_1$, the more usual Ewald construction, e.g. Zachariasen (1945), Schoenborn

(1983), involves (Fig. 1) a single reciprocal lattice and a range of reflecting circles (spheres) of radius $1/\lambda_2$ to $1/\lambda_1$ whose centres, c_2 to c_1 , (and hence the effective location of the specimen crystal, c) are continually displaced as λ changes. This construction

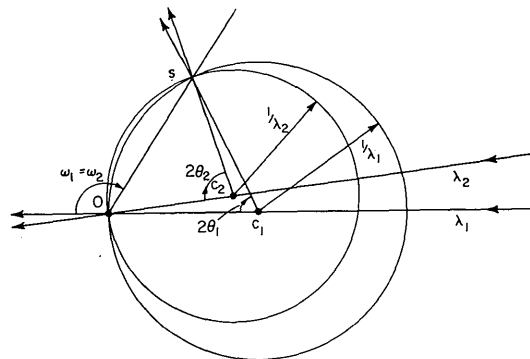


Fig. 1. The interaction of a small single crystal with monochromated X-radiation corresponding to a wavelength band, $\Delta\lambda = \lambda_2 - \lambda_1$, demonstrated by an Ewald construction based on a single reciprocal lattice, origin O , and a range of reflecting circles of radius $1/\lambda_2$ to $1/\lambda_1$, with centres c_2 to c_1 . The point s corresponds to the 'focusing' condition.